Appendix SI.

Materials and methods

Reagents and materials. Written consent was obtained from participants and peripheral blood mononuclear cells (PBMC) from healthy patients were isolated from peripheral blood using Lymphoprep™ reagents (cat. no. 07861; Thermo Fisher Scientific, Inc.). The age range of the healthy PBMC donors enrolled in te present study have the age was 21-30 years old, and the peripheral blood was collected during the period of 2020-2021 at Department of Hematology, Peking University Shenzhen Hospital. Human hematopoietic stem cells (HSC) were isolated from healthy PBMC cells using the EasySep™ Human Progenitor Cell Enrichment Kit with Platelet Depletion (ca.t no. 19356), and the human NK cells were isolated from healthy PBMC cells using the EasySep™ Human NK Cell Isolation Kit from Stem Cell Technologies according to manufacturers instructions. Some of PBMC, NK or isolated healthy HSC were conditionally immortalized using hTERT lentivirus vector with an extended life span to achieve a higher transfection efficiency and experimental stability (1,2). The tumor cell lines, including B95-8, Namalwa, HANK1, and SNK6 cells, were purchased from the American Type Culture Collection and cultured in RPMI-1640 medium containing 2 mmol/l glutamine supplemented with 100 U/ml penicillin, 100 μg/ml streptomycin, 10% human serum and 1,000 U/ml recombinant human IL-2. All cells were maintained in a humidified incubator with 5% CO_2 at 37˚C. The B95-8 cell line was used for EBV viral production and subsequent concentration for the infection of HSC, PBMC or NK cells according to a previously described protocol (3). The EBV LMP1 adenovirus for LMP1 transient infection and related empty control adenovirus were kindly provided by Dr Haimou Zhang from Hubei University.

Antibodies for β-actin (cat. no. sc-47778), C/EBPα (cat. no. sc-365318), CdxA (Cdx1; cat. no. sc-515146), Ets1 (c-ets; cat. no. sc-55581), FOXD3 (HFH2; cat. no. sc-517206), GABPα (cat. no. sc-28312), GATA1 (cat. no. sc-265), GATA2 (cat. no. sc-267), Ki-67 (cat. no. sc-101861), NRF1 (cat. no. sc-101102), NFκB p65 (cat. no. sc-398442) and Oct1 (cat. no. sc-8024) were obtained from Santa Cruz Biotechnology, Inc. Antibodies for acetyl-histone H4 K5, K8, K12, and K16 (H4K5,8,12,16ac; cat. no. PA5-40084) were obtained from Invitrogen; Thermo Fisher Scientific, Inc. Antibodies for DRP1 (cat. no. ab140494), Optic atrophy 1 (OPA1; cat. no. ab157457), Mitofusin 2 (MFN2; cat. no. ab56889), histone H3 acetyl K9, K14, K18, K23, K27 (H3K9,14,18,23,27ac; cat. no. ab47915), H4K20me1 (cat. no. ab9051), H4K20me3 (cat. no. ab9053), H4R3me1 (cat. no. ab17339), H3K9me2 (cat. no. ab1220), H3K9me3 (cat. no. ab8898), H3K27me2 (cat. no. ab24684), H3K27me3 (cat. no. ab6002), H2AX (cat. no. ab20669), γH2AX (cat. no. ab2893) and PGC1β (cat. no. ab240188) were obtained from Abcam. The antibodies for EBV LMP1 (cat. no. NBP1-79009) and 8-oxo-dG (cat. no. 4354-MC-050) were obtained from Novus Biologicals, LLC. 3-nitrotyrosine (3-NT) was measured using the 3-Nitrotyrosine ELISA Kit (cat. no. ab116691; Abcam), and nuclear extracts were prepared using the NE-PER Nuclear and Cytoplasmic Extraction Reagents Kit (Pierce Biotechnology; Thermo Fisher Scientific, Inc.). Protein concentration was measured using the Coomassie Protein Assay Kit (Pierce Biotechnology; Thermo Fisher Scientific, Inc.) following the manufacturers instructions. The siRNA for GABPα, NRF1 and scrambled control were purchased from Ambion; Thermo Fisher Scientific, Inc., and the target sequences of siRNA were provided in Table SI. The Lipofectamine™ Reagent (Invitrogen; Thermo Fisher Scientific, Inc.) was used for DNA transfection (4).

Construction of human DRP1 reporter plasmid. In order to construct DRP1 reporter plasmids, the DRP1 gene promoter (2 kb upstream of the transcription start site) was amplified from Ensembl gene ID: DNM1L-201 ENST00000266481.10 (for DRP1) by PCR from human genomic DNA and subcloned into the pGL3-basic vector (cat. no. E1751; Promega Corporation) using the restriction sites of Mlu I and Xho I with the following primers: DRP1 forward, 5-gcgc-acgcgt- agt tgg ggc cac agg tat gca-3 (Mlu I) and reverse, 5-atcg- ctcgag- aca gtt cgc ctc ctt cct cct-3 (Xho I). In order to map DRP1 promoter activity, the related deletion promoter constructs were generated by PCR methods and subcloned into the pGL3-basic vector (5).

Preparation of gene knockdown lentivirus. The shRNA lentivirus particles for human PGC1β, human NFκB-p65, LMP1 and non-target control were designed and purchased from MilliporeSigma, and all the shRNA target sequences were provided in Table SI; these lentiviruses were used for infection of tumor cell lines (e.g. SNK6). The positive knockdown cells were selected using 10 μg/ml of puromycin and the stable knockdown cell line was confirmed by reverse transcription-quantitative (RT-q) PCR based on an mRNA decrease of more than 65% compared with the control group (primers in Table SII) (4,6).

RT-qPCR. Total RNA from treated cells was extracted using the RNeasy Micro Kit (Qiagen), and the RNA was reverse transcribed using an Omniscript RT kit (Qiagen). All the primers were designed using Primer 3 Plus software with the Tm at 60˚C, primer size of 21 bp, and product length in the range of 140-160 bp (Table SII). The primers were validated with an amplification efficiency in the range of 1.9-2.1 and the amplified products were confirmed with agarose gel. qPCR was run on iCycler iQ (Bio-Rad Laboratories, Inc.) using the Quantitect SYBR green PCR kit (Qiagen). The PCR was performed by denaturing at 95˚C for 8 min followed by 45 cycles of denaturation at 95˚C, annealing at 60˚C, and extension at 72˚C for 10 sec, respectively. A total of 1 μl of each cDNA was used to measure target genes. β-actin was used as the housekeeping gene for transcript normalization, and the mean values were used to calculate relative transcript levels with the $2^{-\Delta\Delta Cq}$ method per instructions from Qiagen. In brief, the amplified transcripts were quantified by the comparative threshold cycle method using β-actin as a normalizer. Fold changes in gene mRNA expression were calculated as $2^{-\Delta\Delta Cq}$ with CT=threshold cycle, ΔCT=CT (target gene)-CT(β-actin), and the ΔΔCT=ΔCT (experimental)-ΔCT (reference) (5,7).

Luciferase reporter assay. A total of $1.0x10^5$ of cells were seeded in a six-well plate with complete medium to grow until they reached 80% confluence. Cells were then co-transfected using 3 μg of reporter constructs, together with 0.2 μg of

pRL-CMV-Luc *Renilla* plasmid (Promega Corporation). The treated cells were then harvested and the luciferase activity assays were carried out using the Dual-Luciferase™ Assay System (Promega Corporation). The transfection efficiencies were normalized using a co-transfected Renilla plasmid according to manufacturers instructions and the reporter activities for PGC1β and OGG1 were calculated (5).

Chromatin immunoprecipitation (ChIP). Cells were washed and crosslinked using 1% formaldehyde for 20 min and terminated by 0.1 M glycine. Cell lysates were sonicated and centrifuged. A total of 500 μg of protein were pre-cleared by BSA/salmon sperm DNA with preimmune IgG and a slurry of Protein A Agarose beads. Immunoprecipitations were performed with the indicated antibodies, BSA/salmon sperm DNA and a 50% slurry of Protein A agarose beads. Input and immunoprecipitates were washed and eluted before then being incubated with 0.2 mg/ml Proteinase K for 2 h at 42˚C, followed by 6 h at 65˚C to reverse the formaldehyde crosslinking. DNA fragments were recovered through phenol/chloroform extraction and ethanol precipitation. A ~150 bp fragment on the related promoter was amplified by real-time PCR (qPCR) using the primers provided in Table SII (5,7).

Western blotting. Cells were lysed in an ice-cold lysis buffer (0.137 M NaCl, 2 mM EDTA, 10% glycerol, 1% NP-40, 20 mM Tris base, pH 8.0) with protease inhibitor cocktail (MilliporeSigma). The proteins were separated in 10% SDS-PAGE and transferred to the PVDF membrane, which was then blotted using primary antibodies (1:1,000) and then simultaneously incubated with the differentially labeled species-specific secondary antibodies, anti-RABBIT IRDye™ 800CW (green) and anti-MOUSE (or goat) ALEXA680 (red). Membranes were scanned and quantitated using the ODYSSEY Infrared Imaging System (LI-COR Biosciences) (8).

Immunostaining. The treated SNK6 cells were transferred to cover slips coated with 0.1% gelatin, fixed by 3.7% formaldehyde at 37˚C for 15 min, permeabilized by 1% BSA + 0.2% Triton X-100 in PBS for 1 h, and then blotted with 40 μg/ml (dilute 1:50) of either PGC1β, Ki-67 (MIB-1) or 8-oxo-dG monoclonal antibodies for 2 h. In some triple staining experiments, the live cells were stained with MitoTracker green before fixation. The cells were then washed three times and the FITC/Texas Red labeled anti-mouse/rabbit secondary antibody (1:100) was added for blotting for another 1 h. After thorough washing, the slides were visualized and photographed; cell nuclei were stained with 4,6-diamidino-2-phenylindole dihydrochloride (DAPI; cat. no. D9542; MilliporeSigma) and the staining was quantitated by ImageJ 1.52v software (National Institutes of Health).

Measurement of oxidative stress. Treated cells were seeded in a 24-well plate and incubated with 10 μM CM-H2DCFDA (Invitrogen; Thermo Fisher Scientific, Inc.) for 45 min at 37˚C; intracellular formation of reactive oxygen species (ROS) was then measured at excitation/emission wavelengths of 485/530 nm using a FLx800 microplate fluorescence reader (Omega Bio-Tek, Inc.), and the data was normalized as arbitrary units (5,9). 3-nitrotyrosine (3-NT) was measured using a 3-Nitrotyrosine ELISA Kit (cat. no. ab116691; Abcam) according to the manufacturer's instructions.

Measurement of DNA breaks. 8-OHdG formation was measured using an OxiSelect™ Oxidative DNA Damage ELISA Kit (cat no. STA320; Cell Biolabs Inc.) according to the manufacturers instructions. The formation of γH2AX was measured from nuclear extracts by western blotting using H2AX as the input control (5).

Measurement of apoptosis. Apoptosis was evaluated by TUNEL assay using the *in situ* Cell Death Detection Kit™ (Roche Diagnostics). Cells were fixed in 4% paraformaldehyde and labeled with TUNEL reagents. Images of the stained cells were captured using a fluorescence microscope and further quantified by FACS analysis (9).

Measurement of mitochondrial function

Mitochondrial DNA copies. Genomic DNA was extracted from treated MM.1R cells using a QIAamp DNA Mini Kit (Qiagen) and the mitochondrial DNA was extracted using the REPLI-g Mitochondrial DNA Kit (Qiagen). The purified DNA was used for the analysis of genomic β-actin (marker of the nuclear gene) and ATP6 (ATP synthase F0 subunit 6, marker of the mitochondrial gene) respectively using the qPCR method as mentioned above. The primers for genomic β-actin are as follows: forward 5-ctg gac ttc gag caa gag atg-3 and reverse: 5-agg aag gaa ggc tgg aag agt-3. Primers for ATP6: forward 5-cat tta cac caa cca ccc aac-3 and reverse 5-tat ggg gat aag ggg tgt agg-3. The mitochondrial DNA copies were obtained from relative ATP6 copies that were normalized by β-actin copies using the $2^{-\Delta\Delta C}$q method (4,7,9).

Intracellular ATP level. The intracellular ATP level was determined using the luciferin/luciferase-induced bioluminescence system. An ATP standard curve was generated at concentrations of 10^{-12}-10^{-3}M. Intracellular ATP levels were calculated and expressed as nmol/mg protein (4,7,9).

Mitochondria membrane potential. Mitochondrial membrane potential (MMP, $\Delta\psi$m) was measured using TMRE (from Molecular Probes T-669) staining. A 600 μM T-669 stock solution was prepared using DMSO. Cells were grown on coverslips and immersed in 600 nM TMRE for 20 min at 37˚C to load them with dye. The labeling medium was then aspirated and the cells were immersed in 150 nM TMRE to maintain the equilibrium distribution of the fluorophore. The coverslips were mounted with live cells onto confocal microscopes to image the cells using 548 nm excitation/573 nm emission filters. The intensity of TMRE fluorescence was measured using ImageJ software. Data from 10-20 cells were collected for each experimental condition and mean values of fluorescence intensity ± SEM were calculated (2,4,5).

Mitochondria morphology by electron microscopy. Treated cells were harvested and fixed by 2.5% glutaraldehyde, then dehydrated by a series of increased concentrations of ethanol and embedded in epoxy resin and propylene oxide overnight. The 70 nm-thick sample sections were then stained by lead citrate, and the mitochondrial morphology was detected under a transmission electron microscope by double-blinded technicians (10).

DNA methylation analysis. A real-time PCR-based method was developed for methylation-specific PCR (MSP) analysis on the human PGC1β promoter according to the previously described method with some modifications (11-13). Genomic DNA from treated human tumor cells was extracted and purified before being treated by bisulfite modification using the EpiJET Bisulfite Conversion kit (cat. no. K1461; Thermo Fisher Scientific, Inc.). The modified DNA was amplified using methylated and unmethylated primers for MSP that were designed using the Methprimer software: (http://www.urogene.org/cgi-bin/methprimer/methprimer.cgi) with the following details: Methylated primer: forward 5-ttt tta aag tgt tgg gat tat agg c-3, reverse 5-acg tta cgt taa cgc taa acg a-3; unmethylated primer: forward 5-ttt aaa gtg ttg gga tta tag gtg t-3, reverse 5-tca cat tac att aac act aaa caa a-3. The product sizes were as follows: 142 bp (methylated) with Tm: 66.4˚C & 142 bp (unmethylated) with Tm: 65.8˚C; CpG island size: 197 bp; The final methylation readout was normalized by unmethylated input PCR (7).

Detection of EBV copy number. Genomic DNA was extracted from treated tumor cell lines using a QIAamp DNA Mini Kit (Qiagen). The EBV DNA copy number was measured through qPCR using 50 ng of total DNA with EBV BMRF1 primers (Table SII), and the results were normalized using cellular β-actin (primers see Table SII) as an internal control (14,15). The Namalwa cell line, which contains 2 EBV viral genome copies, was used as a standard to prepare calibration curves for both EBV BMRF1 and β-actin genes, and the EBV viral load was presented as the number of viral genomes per cell (16,17).

[^{3}H]-deoxyglucose uptake. A total of 1x10^6 treated cells were suspended and rinsed with PBS three times and were then incubated with 1 ml of PBS containing 1.0 μCi 3H-deoxyglucose for 5 min at 37˚C. Cells were washed three times with cold PBS and then solubilized in 1 ml of 1M NaOH for 60 min at 37˚C. They were then neutralized with an equal volume of 1 M HCl and counted in 10 ml scintillation mixture, and the final results were normalized by protein level.

DNA synthesis by [^{3}H]-thymidine incorporation. Cell proliferation was evaluated as the rate of DNA synthesis by [^{3}H]-methylthymidine incorporation (18). Cells were pooled in 24-well plates until they reached 80% confluence; the indicated chemicals were then added and incubated for 24 h. At the end of the treatment, cells were incubated with serum-free media containing ^{3}H-methylthymidine (0.5 μCi/well) for 2 h and then washed twice with PBS. Cellular DNA was precipitated using 10% trichloroacetic acid and solubilized with 0.4 M NaOH (0.5 ml/well). Incorporation of ^{3}H-methylthymidine into the DNA was measured in a scintillation counter and determined in the units of counts per min (CPM) (5).

Colony formation in soft agar. This assay is a method for evaluating the ability of individual cell lines to grow in an anchorage-independent manner. Cells were resuspended in DMEM containing 5% FBS with 0.3% agarose and layered on top of 0.5% agarose in DMEM on 60-mm plates. A total of 1,000 cells were seeded in 60 mm soft agar dishes for 30 days. The dishes were examined twice per week, and colonies that grew beyond 50 mm in diameter were scored as positive. Each experiment was performed in quadruplicate (5).

In vivo mouse experiments. Balb/c athymic nude male mice (6 weeks old) were obtained from the Guangdong Medical Animal Center. All procedures involving mice were conducted in accordance with NIH regulations concerning the use and care of experimental animals and were approved by the Institutional Animal Care and Use Committee of Peking University Shenzhen Hospital. A total of 2x10^6 of viable treated tumor cells were washed, harvested in PBS, and then injected into the lateral tail vein in a volume of 0.1 ml. The tail vein injection with a standard restrainer was routinely performed on conscious mice in our lab, no anesthesia was given. The mice receiving tail vein injections were separated into the following 4 groups (n=9). Group 1 (CTL): conditionally immortalized HSC cells at passage #6 after vehicle lentivirus infection; Group 2 (EBV): conditionally immortalized HSC cells at passage #6 after EBV infection; Group 3 (LMP↑): conditionally immortalized HSC cells at passage #6 after LMP1 adenovirus infection; Group 4 (EBV/shPGC1β): conditionally immortalized HSC cells at passage #6 after EBV infection and shPGC1β lentivirus infection in the presence of 10 μg/ml puromycin.

Mice were monitored for changes in body weight and euthanized by cervical dislocation when values fell below 20% of their initial weight. The survival curve was calculated and the final tumor tissues were isolated for biomedical analysis. The lungs of sacrificed mice were isolated and fixed in 10% formalin and the number of surface metastases per lung was determined under a dissecting microscope. Parts of the tumor tissues were fixed in 4% buffered formaldehyde, paraffin embedded, and sectioned to 4 mm thickness before they were then processed for H&E staining. Images were captured using a Carl Zeiss MIRAX MIDI slide scanner and analyses were performed using a 3DHISTECH Pannoramic Viewer. Parts of the tumor tissues were isolated for *in vivo* monitoring of superoxide anion release; gene expression was measured through real time PCR for mRNA and western blotting was used for protein levels (4,5,19).

In vivo superoxide anion ($O_2^{\cdot-}$) release. Superoxide anion release in amygdala tissues was extracted by dimethyl sulfoxide-tetrabutylammonium chloride (DMSO-TBAC) solution and the TBAC-$O_2^{\cdot-}$ complex was then further detected by use of the luminol-EDTA-Fe enhanced chemiluminescence system (20). Briefly, the biological tissues were isolated and purged continuously by N_2 gas to remove traces of oxygen, and $O_2^{\cdot-}$ from tissues was extracted by DMSO-TBAC, then the chemiluminescent reagents and $O_2^{\cdot-}$ extract solutions were pumped into a glass scintillation vial which was placed in the luminometer, and the chemiluminescence intensity was continuously monitored for 2 min and calculated. Superoxide levels were calculated from the standard curve generated by the xanthine/xanthine oxidase reaction (9).

Statistical analysis. The data was presented as the mean ± SD; all of the experiments were performed at least in quadruplicate unless otherwise indicated. The data was analyzed as normal distribution using Shapiro-Wilk test to evaluate the normality

of the data in SPSS 22 software (21), and the one-way analysis of variance (ANOVA) followed by the Tukey-Kramer test was used to determine statistical significance of different groups. The mouse survival curve was determined through Kaplan-Meier survival analysis using SPSS 22 software (IBM Corp.), and a $P<0.05$ was considered to indicate a statistically significant difference (5).

References

1. Bodnar AG, Ouellette M, Frolkis M, Holt SE, Chiu CP, Morin GB, Harley CB, Shay JB, Lichtsteiner S and Wright WE: Extension of life-span by introduction of telomerase into normal human cells. Science 279: 349-352, 1998.
2. Kong D, Zhan Y, Liu Z, Ding T, Li M, Yu H, Zhang L, Li H, Luo A, Zhang D, *et al*: SIRT1-mediated ERβ suppression in the endothelium contributes to vascular aging. Aging Cell 15: 1092-1102, 2016.
3. Lan K, Verma SC, Murakami M, Bajaj B and Robertson ES: Epstein-Barr Virus (EBV): infection, propagation, quantitation, and storage. Curr Protoc Microbiol. Chapter 14:Unit 14E.2, 2007.
4. Zhang H, Li L, Chen Q, Li M, Feng J, Sun Y, Zhao R, Zhu Y, Lv Y, Zhu Z, *et al*: PGC1β regulates multiple myeloma tumor growth through LDHA-mediated glycolytic metabolism. Mol Oncol 12: 1579-1595, 2018.
5. Zhang H, Li L, Li M, Huang X, Xie W, Xiang W and Yao P: Combination of betulinic acid and chidamide inhibits acute myeloid leukemia by suppression of the HIF1α pathway and generation of reactive oxygen species. Oncotarget 8: 94743-94758, 2017.
6. Chen X, Lv Y, Sun Y, Zhang H, Xie W, Zhong L, Chen Q, Li M, Li L, Feng J, *et al*: PGC1β regulates breast tumor growth and metastasis by SREBP1-mediated HKDC1 expression. Front Oncol 9: 290, 2019.
7. Zou Y, Lu Q, Zheng D, Chu Z, Liu Z, Chen H, Ruan Q, Ge X, Zhang Z, Wang X, *et al*: Prenatal levonorgestrel exposure induces autism-like behavior in offspring through ERβ suppression in the amygdala. Mol Autism 8: 46, 2017.
8. Ceradini DJ, Yao D, Grogan RH, Callaghan MJ, Edelstein D, Brownlee M and Gurtner GC: Decreasing intracellular superoxide corrects defective ischemia-induced new vessel formation in diabetic mice. J Biol Chem 283: 10930-10938, 2008.
9. Yao D, Shi W, Gou Y, Zhou X, Yee Aw T, Zhou Y and Liu Z: Fatty acid-mediated intracellular iron translocation: A synergistic mechanism of oxidative injury. Free Radic Biol Med 39: 1385-1398, 2005.
10. Gong L-J, Wang X-Y, Gu W-Y and Wu X: Pinocembrin ameliorates intermittent hypoxia-induced neuroinflammation through BNIP3-dependent mitophagy in a murine model of sleep apnea. J Neuroinflammation 17: 337, 2020.
11. Ogino S, Kawasaki T, Brahmandam M, Cantor M, Kirkner GJ, Spiegelman D, Makrigiorgos GM, Weisenberger DJ, Laird PW, Loda M and Fuchs CS: Precision and performance characteristics of bisulfite conversion and real-time PCR (MethyLight) for quantitative DNA methylation analysis. J Mol Diagn 8: 209-217, 2006.
12. Eads CA, Danenberg KD, Kawakami K, Saltz LB, Blake C, Shibata D, Danenberg PV and Laird PW: MethyLight: A high-throughput assay to measure DNA methylation. Nucleic Acids Res 28: E32, 2000.
13. Nosho K, Irahara N, Shima K, Kure S, Kirkner GJ, Schernhammer ES, Hazra A, Hunter DJ, Quackenbush J, Spiegelman D, *et al*: Comprehensive biostatistical analysis of CpG island methylator phenotype in colorectal cancer using a large population-based sample. PLoS ONE 3: e3698, 2008.
14. Verma D, Thompson J and Swaminathan S: Spironolactone blocks Epstein-Barr virus production by inhibiting EBV SM protein function. Proc Natl Acad Sci USA 113: 3609-3614, 2016.
15. Zuo L, Yu H, Liu L, Tang Y, Wu H, Yang J, Zhu M, Du S, Zhao L, Cao L, *et al*: The copy number of Epstein-Barr virus latent genome correlates with the oncogenicity by the activation level of LMP1 and NF-κB. Oncotarget 6: 41033-41044, 2015.
16. Hui KF and Chiang AKS: Suberoylanilide hydroxamic acid induces viral lytic cycle in Epstein-Barr virus-positive epithelial malignancies and mediates enhanced cell death. Int J Cancer 126: 2478-2489, 2010.
17. Rose C, Green M, Webber S, Kingsley L, Day R, Watkins S, Reyes J and Rowe D: Detection of Epstein-Barr virus genomes in peripheral blood B cells from solid-organ transplant recipients by fluorescence in situ hybridization. J Clin Microbiol 40: 2533-2544, 2002.
18. Somasundaram K and El-Deiry WS: Inhibition of p53-mediated transactivation and cell cycle arrest by E1A through its p300/CBP-interacting region. Oncogene 14: 1047-1057, 1997.
19. Zhang H, Lu J, Jiao Y, Chen Q, Li M, Wang Z, Yu Z, Huang X, Yao A, Gao Q, *et al*: Aspirin inhibits natural killer/T-cell lymphoma by modulation of VEGF expression and mitochondrial function. Front Oncol 8: 679, 2018.
20. Yao D, Vlessidis AG, Gou Y, Zhou X, Zhou Y and Evmiridis NP: Chemiluminescence detection of superoxide anion release and superoxide dismutase activity: Modulation effect of Pulsatilla chinensis. Anal Bioanal Chem 379: 171-177, 2004.
21. Ramezani G, Norouzi A, Arabshahi SKS, Sohrabi Z, Zazoli AZ, Saravani S and Pourbairamian G: Study of medical students learning approaches and their association with academic performance and problem-solving styles. J Educ Health Promot 11: 252, 2022.

Figure S1. Representative western blot images. (A) Representative full blots of Fig. 1B. (B) Representative full blots of Fig. 3C. (C) Representative full blots of Fig. 4D. (D). Representative full blots of Fig. 5J. (E) Representative full blots of Fig. 7B.

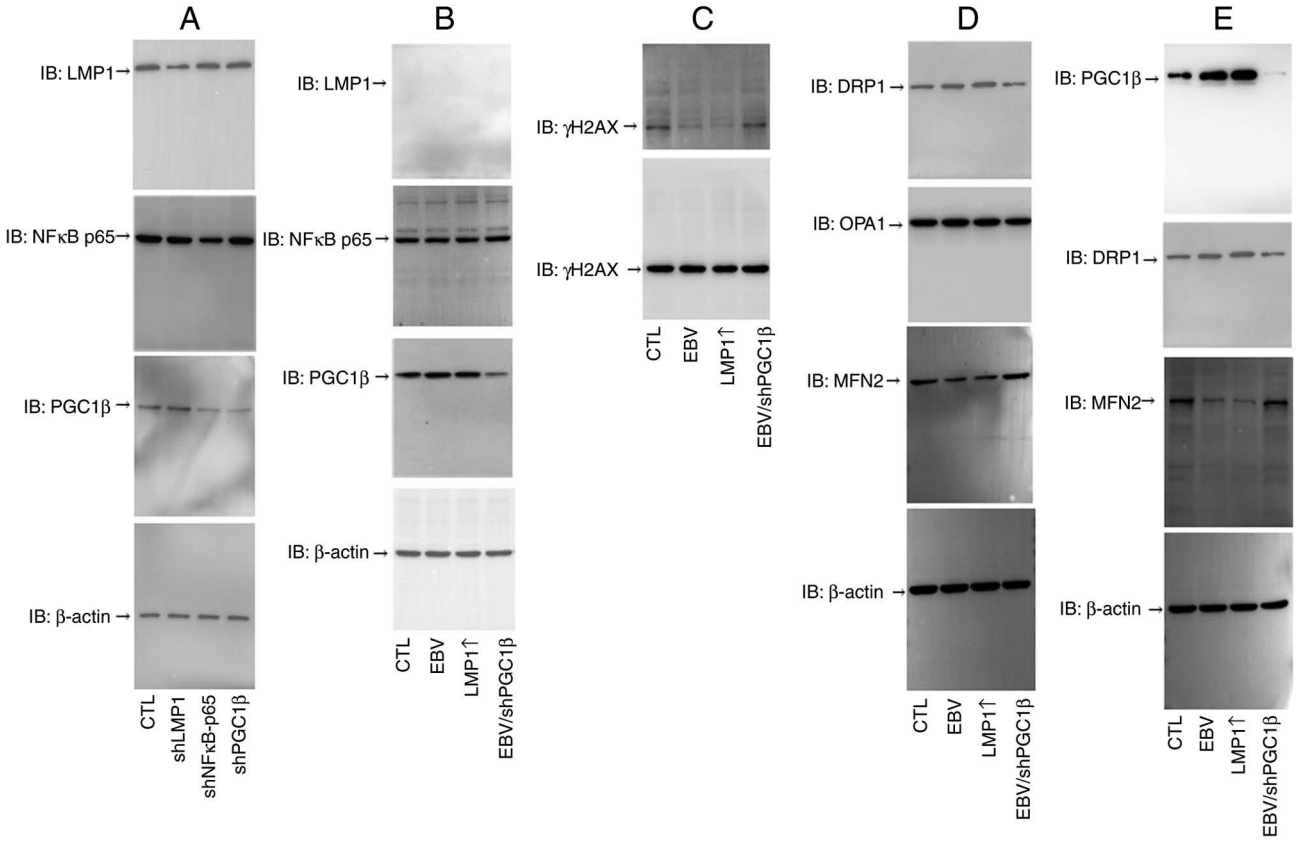

Figure S2. LMP1 knockdown in Epstein-Barr virus-positive tumor cells does not affect PGC1β expression. Tumor cells were treated with CTL, shLMP1, sh nuclear factor-κB-p65 or shPGC1β lentivirus, and the cells were then harvested for biomedical analysis. (A) mRNA levels in HANK1 cells (n=4). (B) mRNA levels in SNT8 cells (n=4). *P<0.05 vs. CTL group. LMP1, latent membrane protein 1; PGC1β, peroxisome proliferator-activated receptor-γ coactivator-1β; CTL, control; sh, short hairpin.

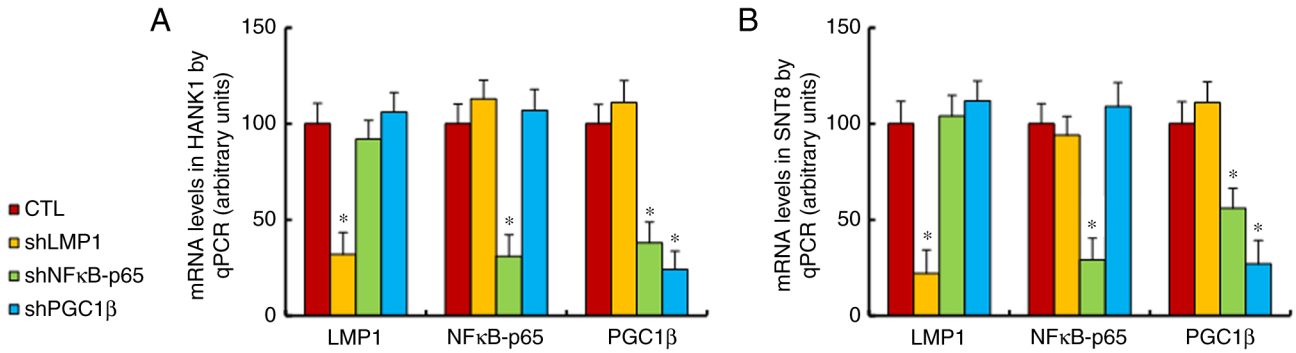

Figure S3. Knockdown of the LMP1/NF-κB-p65/PGC1β signaling pathway in Epstein-Barr virus-positive tumor cells does not affect epigenetic changes on the PGC1β promoter. SNK6 tumor cells were treated with control, shLMP1, shNFκB-p65, or shPGC1β lentivirus, and the cells were then harvested for chromatin immunoprecipitation analysis. (A) Histone H3 methylation on the PGC1β promoter (n=4). (B) DNA methylation on the PGC1β promoter (n=4). (C) Histone acetylation on the PGC1β promoter using anti-H3K9,14,18,23,27ac and anti-H4K5,8,12,16ac antibodies (n=4). (D) Histone H4 methylation on the PGC1β promoter (n=4). LMP1, latent membrane protein 1; PGC1β, peroxisome proliferator-activated receptor-γ coactivator-1β; NF-κB; nuclear factor-κB; sh, short hairpin.

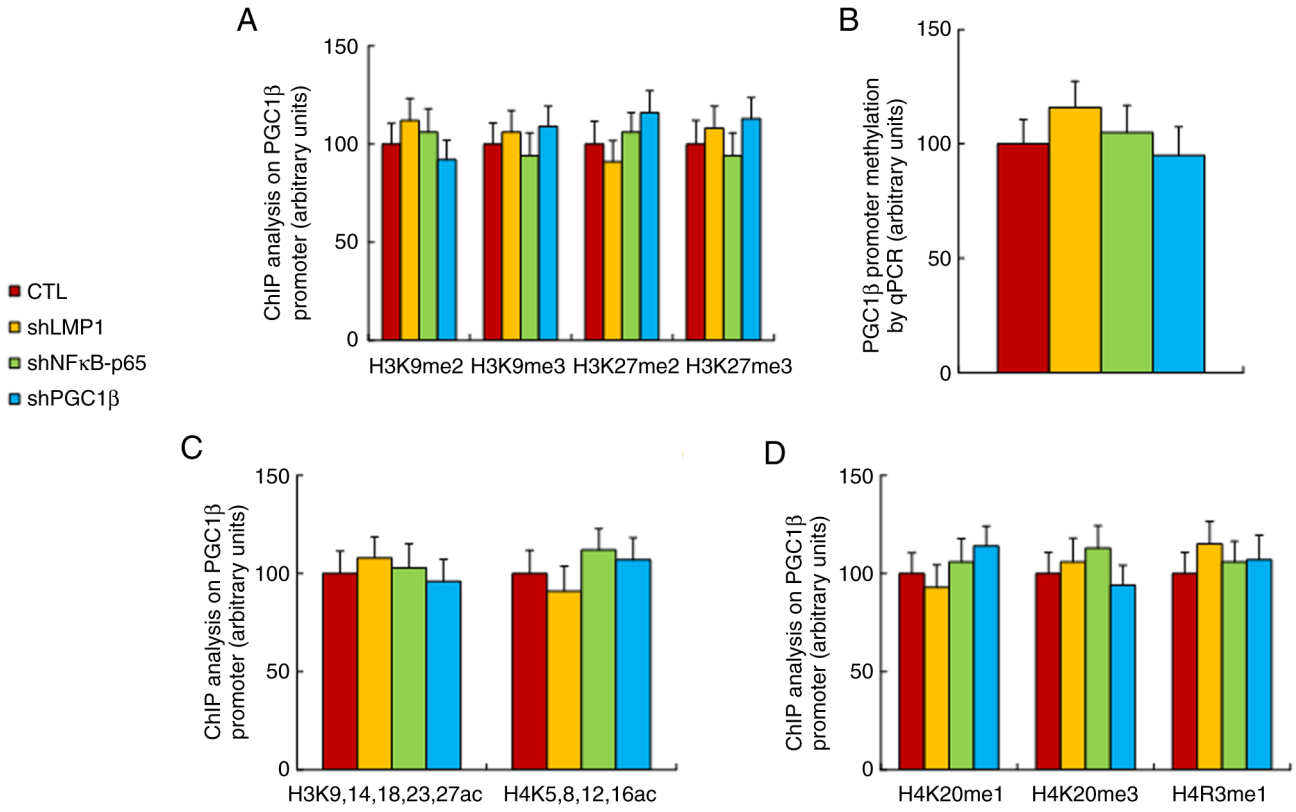

Figure S4. EBV/LMP1 expression causes epigenetic modifications on the PGC1β promoter. Conditionally immortalized hematopoietic stem cells were infected by CTL, EBV, LMP1 adenovirus infection (LMP1↑) or EBV together with shPGC1β lentivirus in the presence of 10 μg/ml puromycin (EBV/shPGC1β), and the cells were harvested for biomedical analysis at passage #1. (A) EBV DNA genomic copies (n=5). (B) mRNA levels, as determined by quantitative PCR (n=4). (C) Histone H3 methylation on the PGC1β promoter (n=4). (D) DNA methylation on the PGC1β promoter (n=4). (E) Histone acetylation on the PGC1β promoter using anti-H3K9,14,18,23,27ac and anti-H4K5,8,12,16ac antibodies (n=4). (F) Histone H4 methylation on the PGC1β promoter (n=4). *P<0.05 vs. CTL group. EBV, Epstein-Barr virus; LMP1, latent membrane protein 1; PGC1β, peroxisome proliferator-activated receptor-γ coactivator-1β; CTL, control; sh, short hairpin.

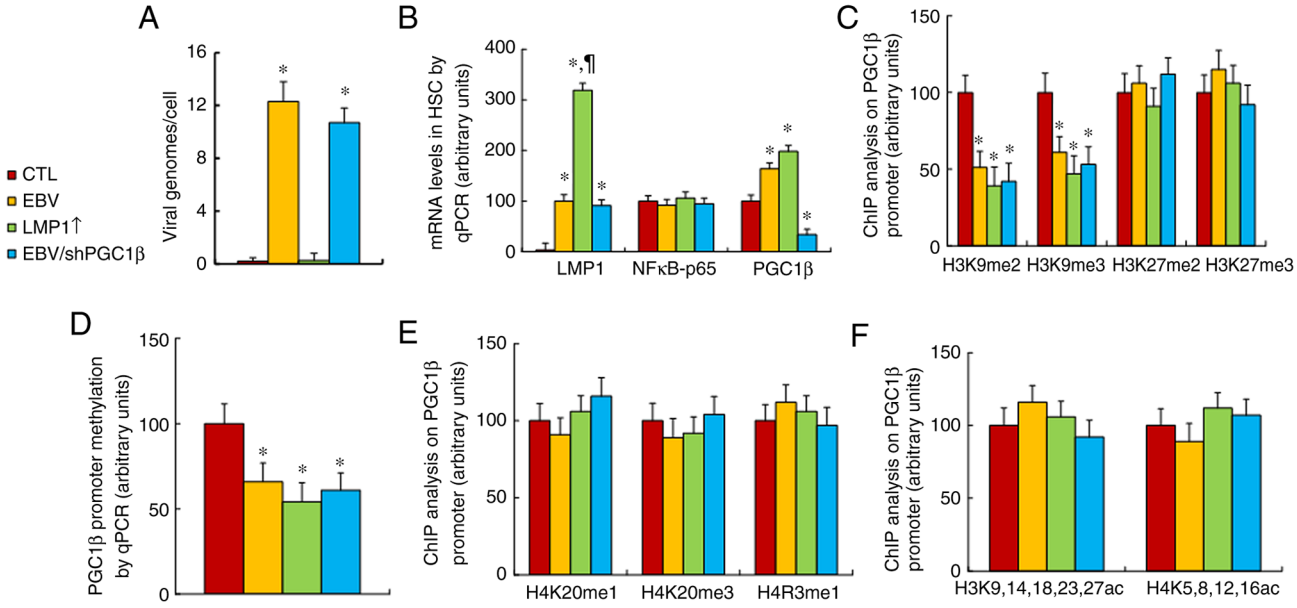

Figure S5. EBV/LMP1 expression-mediated epigenetic modifications on the PGC1β promoter. Conditionally immortalized hematopoietic stem cells were infected with control, EBV, LMP1 adenovirus infection (LMP1↑) or EBV together with shPGC1β lentivirus in the presence of 10 μg/ml puromycin (EBV/shPGC1β). The cells were continuously cultured, and then harvested for biomedical analysis at passage #6. (A) Histone acetylation on the PGC1β promoter using anti-H3K9,14,18,23,27ac and anti-H4K5,8,12,16ac antibodies (n=4). (B) Histone H4 methylation on the PGC1β promoter (n=4). EBV, Epstein-Barr virus; LMP1, latent membrane protein 1; PGC1β, peroxisome proliferator-activated receptor-γ coactivator-1β; sh, short hairpin.

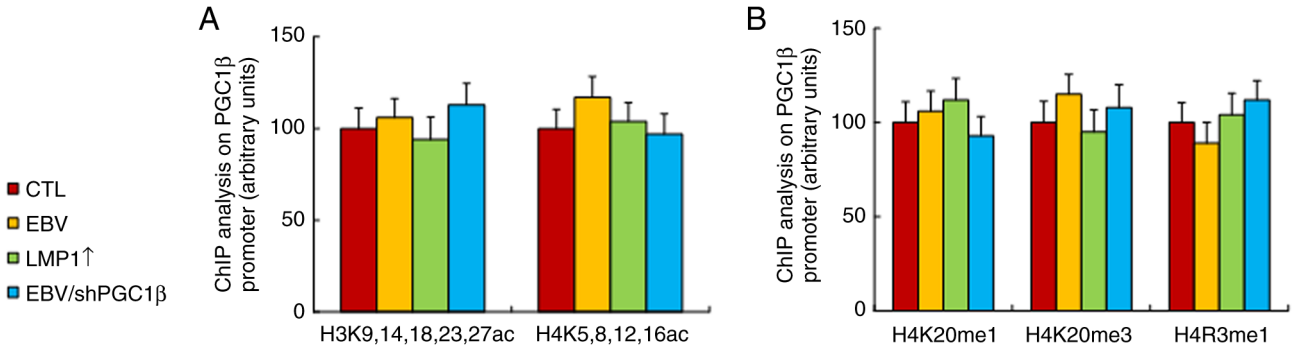

Figure S6. EBV/LMP1 expression causes persistent PGC1β upregulation in different cells. Conditionally immortalized cells were infected with CTL, EBV, LMP1 adenovirus (LMP1↑)or EBV virus together with shPGC1β lentivirus in the presence of 10 μg/ml puromycin (EBV/shPGC1β). The cells were continuously cultured, and then harvested for PCG1β mRNA analysis at different passages (from #1 to #6). (A) PCG1β mRNA level in peripheral blood mononuclear cells (n=4). (B) PCG1β mRNA level in natural killer cells (n=4). *P<0.05 vs. CTL group. EBV, Epstein-Barr virus; LMP1, latent membrane protein 1; PGC1β, peroxisome proliferator-activated receptor-γ coactivator-1β; CTL, control; sh, short hairpin.